ACS APPLIED MATERIALS & INTERFACES

Research Article

www.acsami.org

Piezotronic Interface Engineering on ZnO/Au-Based Schottky Junction for Enhanced Photoresponse of a Flexible Self-Powered UV Detector

Shengnan Lu,[†] Junjie Qi,[†] Shuo Liu,[†] Zheng Zhang,[†] Zengze Wang,[†] Pei Lin,[‡] Qingliang Liao,[†] Qijie Liang,[†] and Yue Zhang*[,†,‡]

[†]State Key Laboratory for Advanced Metals and Materials, School of Materials Science and Engineering, University of Science and Technology Beijing, Beijing 100083, People's Republic of China

[‡]Key Laboratory of New Energy Materials and Technologies, University of Science and Technology Beijing, Beijing 100083, People's Republic of China

ABSTRACT: Exploiting piezoelectric effect to engineer material interface has been confirmed as a promising way to optimize the performance of optoelectronic devices. Here, by using this effect, we have greatly improved the photoresponse of the fabricated ZnO/Au Schottky junction based self-powered UV detector. A 440% augment of photocurrent, together with 5× increased sensitivity, was obtained when the device was subjected to a 0.580% tensile strain. The enhancement can be attributed to the facility separation and extraction of photoexcites due to the formation of the stronger and expanding built-in field, which is a result of charge redistribution induced by piezoelectric polarization at the ZnO/Au interface. This study not only can strengthen the understanding of piezoelectric effects on energy devices but also can be extended to boost performances of optoelectronic devices made of piezoelectric semiconductor materials.

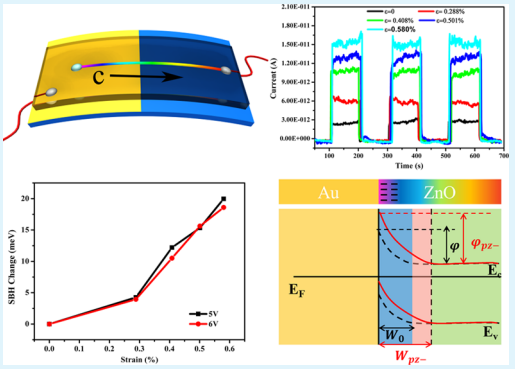

KEYWORDS: *interface engineering, piezopotential, Schottky barrier, ZnO, self-powered, UV detector*

INTRODUCTION

Precisely controlled materials and their interfaces are pivotal determinants of device performance in fundamental science. Particularly, compared to the bulk of materials, the interface is more fascinating and exhibits some unexpected physical properties, such as superlattices, band offsets, or energy barrier formations, which in turn dominate the overall behavior of devices.[1−3] Thus, the performance of the devices is directed mostly by the interface characteristics. Accordingly, interface engineering has aroused considerable attention in optimizing device performance or designing novel functional devices.[4−7] Among the emerging approaches, employing the ionic depolarization induced electric field to regulate the interfacial electronic band structure without varying interfacial structure or chemistry is an intriguing method.[8−20] Nevertheless, considering the poor electrical conductivity of most ferroelectric materials,[8,9] the semiconducting piezoelectric materials are more feasible for constructing electronic devices. Thereinto, ZnO nanomaterial is considered to be an ideal building block for optoelectronic devices in view of its outstanding optoelectric properties and its facile synthesis.[21−24] Additionally, the ability to tailor heterointerface with the piezoelectric polarization has been demonstrated.[12−20]

On the other hand, the self-powered system that performs wirelessly, independently, and sustainably is another hot issue with the threat of the global energy crisis.[25−27] The self-powered ultraviolet (UV) photodetector, one of the most popular optoelectronic devices, has also been developed.[27−35] Different from the nanogenerator or a solar cell integrated self-powered photodetector, which are more or less time-, weather-, and temperature-dependent,[27,28] the photovoltaic-effect-based self-powered photodetector is powered by the detecting signals rather than by another energy collection system, showing greater adaptability and sustainability.[29−35] Generally, there are two types of photovoltaic photodetector: Schottky junction[29−31] and p−n junction.[32−35] As the Schottky type device has the advantage of ease of fabrication processing over the p−n type device, it would be more preferable in practical application and worth spending more time on investigating how to improve its performances.

Though piezopotential boosting photovoltaic effect has been reported,[12−15] there is a little work focused on the Schottky-based photovoltaic device. In this work, the influence of the interfacial remnant piezopotential engineering of a ZnO/Au Schottky junction on its photovoltaic performance is manifested by a self-powered UV detector, where the photocurrent increases linearly with tensile strain. With a 0.580% tensile strain, the photocurrent was further enhanced

Received: June 2, 2014
Accepted: July 28, 2014
Published: July 28, 2014

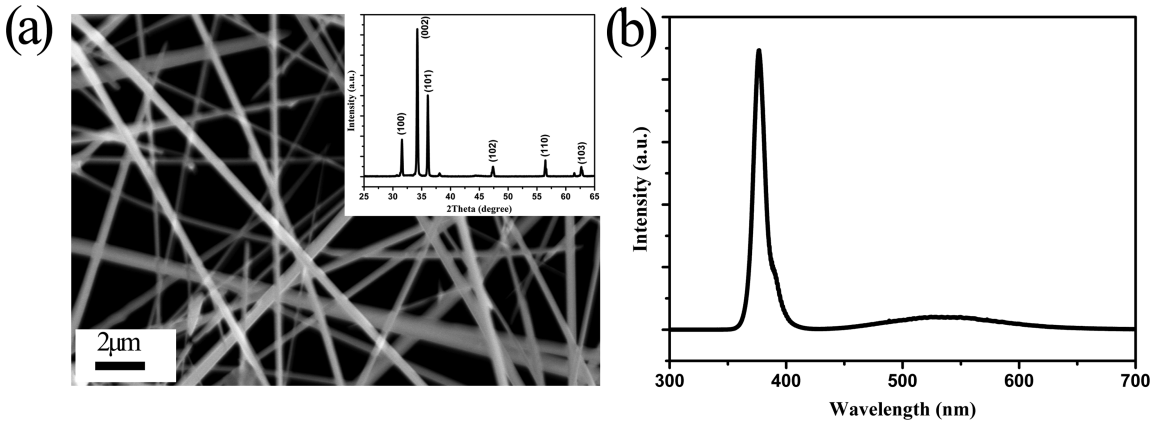

Figure 1. (a) SEM micrograph of the synthesized ZnO wires; (inset) XRD pattern of the ZnO sample. (b) PL spectrum of the ZnO wires.

440% along with a more than 5× improvement of sensitivity. The underlying mechanisms are clarified in terms of energy band diagrams. Our investigation is beneficial to performance optimization of optoelectronic devices and valuable for developing self-powered systems.

EXPERIMENTAL SECTION

As a good Schottky barrier junction is needed for our investigation, a 100 nm Au film acting as an electrode was sputtered on a flexible polystyrene (PS) substrate partially via DC sputtering. The ZnO micro/nanowires investigated in this work were synthesized by a simple chemical vapor deposition method.[36] A selective ZnO wire of large size was transferred on the as-treated PS substrate along the long edge and connected with Au film at one end of the wire to form a Schottky junction. Furthermore, to avoid the movement of the ZnO wire during the testing procedure, we tightly bound the ZnO wire to the Au film with a thin film of epoxy. Then, Ag paste was used to fix the ZnO wire on the PS substrate as an electrode. Finally, a thin layer of polydimethylsiloxane (PDMS) was brought in to fully cover the whole device and isolate the device from contamination.

The morphology and structure of the ZnO wire and the fabricated device were characterized by scanning electron microscope (SEM, JEOL-6490), optical microscope, and X-ray diffractometer (Rigaku DMAX-RB, Japan). The photoluminescence spectrum was obtained using a continuous He−Cd (325 nm) laser as an excitation source, which is also the light source in our work. The room temperature electrical and photoresponse properties of the device were measured with a semiconductor characterization system (Keithley 4200-SCS).

RESULTS AND DISCUSSION

Figure 1a represents a typical SEM image of the synthesized wire. Dense wires with widths of hundreds of nanometers to a few micrometers and lengths of several hundred micrometers can be easily seen. The well matched diffraction peaks of the XRD pattern of the ZnO wire in the inset of Figure 1a indicate the wurtzite structure of our products and no secondary phase.[37] The PL spectrum is also depicted in Figure 1b to assess the crystallinity of the ZnO wires, suggesting good crystallinity with low deficiencies of the as-prepared ZnO wires.[38]

The optical image of the fabricated device is shown in the top image in Figure 2a, and the bottom image is a schematic of the device. To evaluate the electronic properties of the fabricated ZnO/Au heterojunction, we initially recorded the current−voltage (I−V) characteristic. As seen in Figure 2b, the device displays an excellent diode-like behavior with a fairly low turn-on voltage of about 0.25 V and a rectification ratio greater than 10^3 at ±3 V, indicating the well-defined Schottky barrier formed at the ZnO/Au interface. The ideality factor of the ZnO/Au heterojunction derived from the slope of the ln I vs I curve plotted in Figure 2b based on the thermionic emission model is about 3.04,[14] while the ideal one should be 1. The deviation from the ideal value here may ascribe to the electron−hole recombination process because of the surface states at the interface of the heterojunction.[39] Additionally, the capacitance−voltage curve (Figure 2c) was also obtained to show the interface state comprehensively. According to the Mott−Schottky equation,[40] the carrier density and the built-in potential were estimated to be 2.6×10^{17} cm^{-3} and 0.79 V, respectively, through linearly fitting the $1/C^2$ versus voltage curve.

$$\frac{1}{C^2} = \frac{2(\varphi - V)}{A^2 q \varepsilon \varepsilon_0 N_s}$$

where φ is the built-in potential, V is the external applied potential, q is the elementary charge, A is the area of the metal contacts, ε is the dielectric constant, ε_0 is the permittivity of vacuum, and N_s is the carrier concentration. It can be perceived that the ZnO wire is appropriated to investigate piezotronics and to construct piezoelectric devices for its moderate carrier density.[41] The depletion width of about 80 nm at 0 V was further obtained by employing the equation[40]

$$W = \sqrt{\frac{2\varepsilon_s(\varphi - V)}{qN_a}}$$

These results acquired from the CV curve again confirmed that a reliable barrier would be formed at the ZnO/Au interface via this easy and low-cost means.

Furthermore, Figure 2d illustrates the photoresponse property of the device at zero bias. The Schottky junction has remarkable photovoltaic performance, and the current repeatedly increases/decreases stably during periodical switching of light illumination with a sensitivity (defined as photocurrent/dark current) as high as ~10^3. More importantly, there is no distinct degradation in each cycle. The response process was fast, and the corresponding rise and decay times are presented in Figure 2e, which shows both of them are about 0.1 s. The self-powered behavior of our device accompanied by its fast response speed relative to photoconductive photodetectors relies on the driving force of the Schottky barrier at the ZnO/Au interface rather than the oxygen absorption and desorption process at the surface of the ZnO wire, which can be elucidated with the help of the energy band diagram in Figure

dx.doi.org/10.1021/am503442c | ACS Appl. Mater. Interfaces 2014, 6, 14116−14122

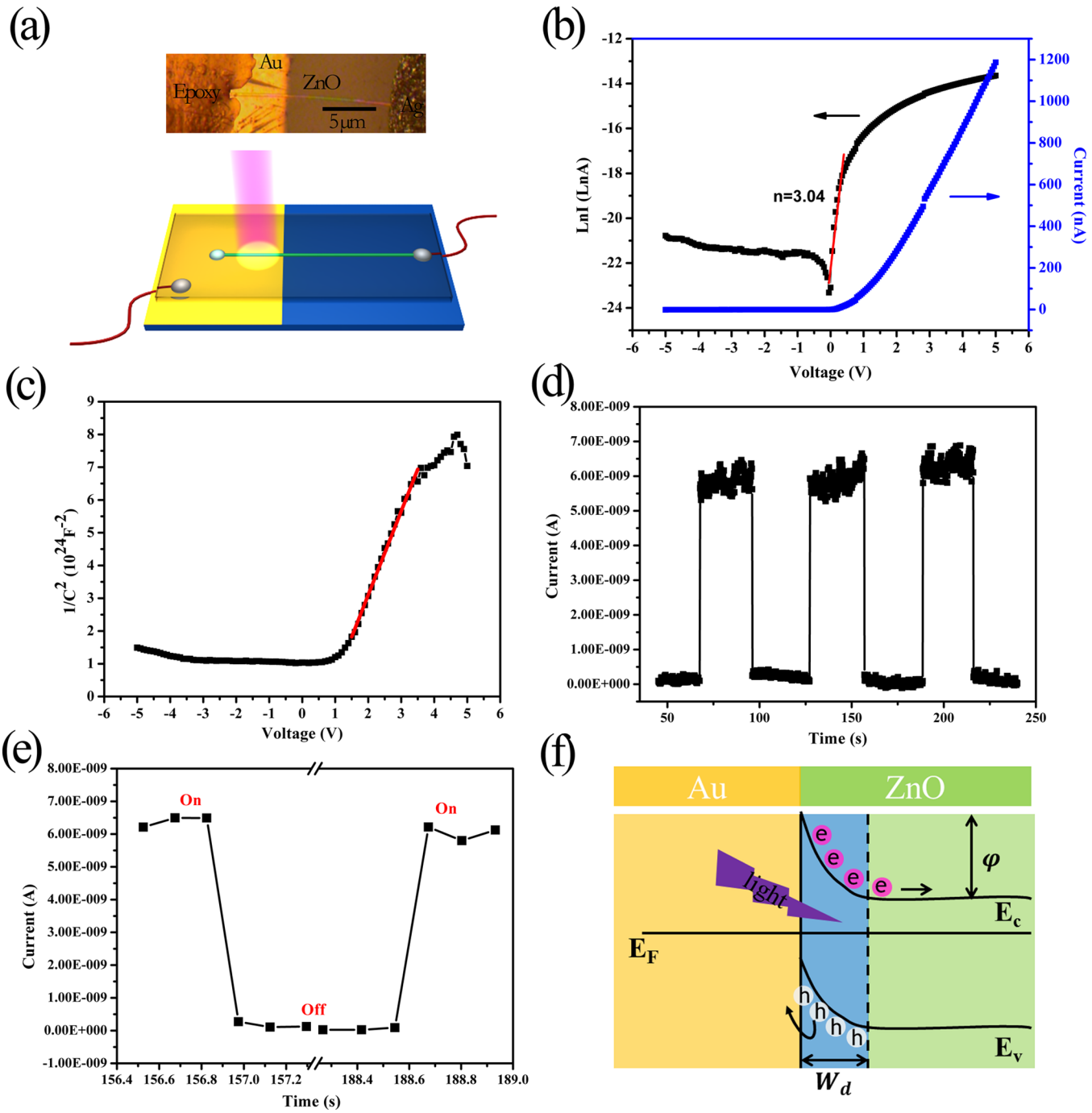

Figure 2. (a, top) Optical image and (a, bottom) schematic of the fabricated device. (b) Linear and semilogarithmic plot of current and voltage, respectively. (c) The *C*−*V* characteristic of the ZnO/Au junction. (d) Time-resolve photoresponse of the fabricated device under UV irritation (325 nm). (e) The rise and decay time enlarged. (f) Schematic band structure of the Schottky barrier under UV illumination.

2f. It is well-known that there is a built-in potential at the metal/n-semiconductor interface when the work function of the semiconductor is lower than that of the metal, such as ZnO (4.5 eV) and Au (5.1 eV),[31] thus leading to the band distortion and the formation of the depletion region adjacent to the interface. Once the junction is illuminated by the above-band gap light (325 nm), the electrons and holes generated within the depletion region are immediately driven in opposite directions by the built-in potential, which gives rise to the generation of the circuit current.

Owing to the modulation of the interface band structure originated from piezoelectric polarization,[12−18] the photoresponse performance of the ZnO/Au Schottky junction under different strains is systematically investigated because of the dominant effect of the interface characteristics, as described above and summarized in Figure 3. The output current increases step by step as the tensile strain gradually increases, which could be introduced and calculated by applying different curvatures on the PS substrate.[14] Meanwhile, at each strain state, the signal current would return to a steady value once the light irradiation is on or off in each cycle with a nearly unchangeable rise and decay time. To further understand the strain effect on the device performance, we extracted the photocurrent and the sensitivity under different strains from

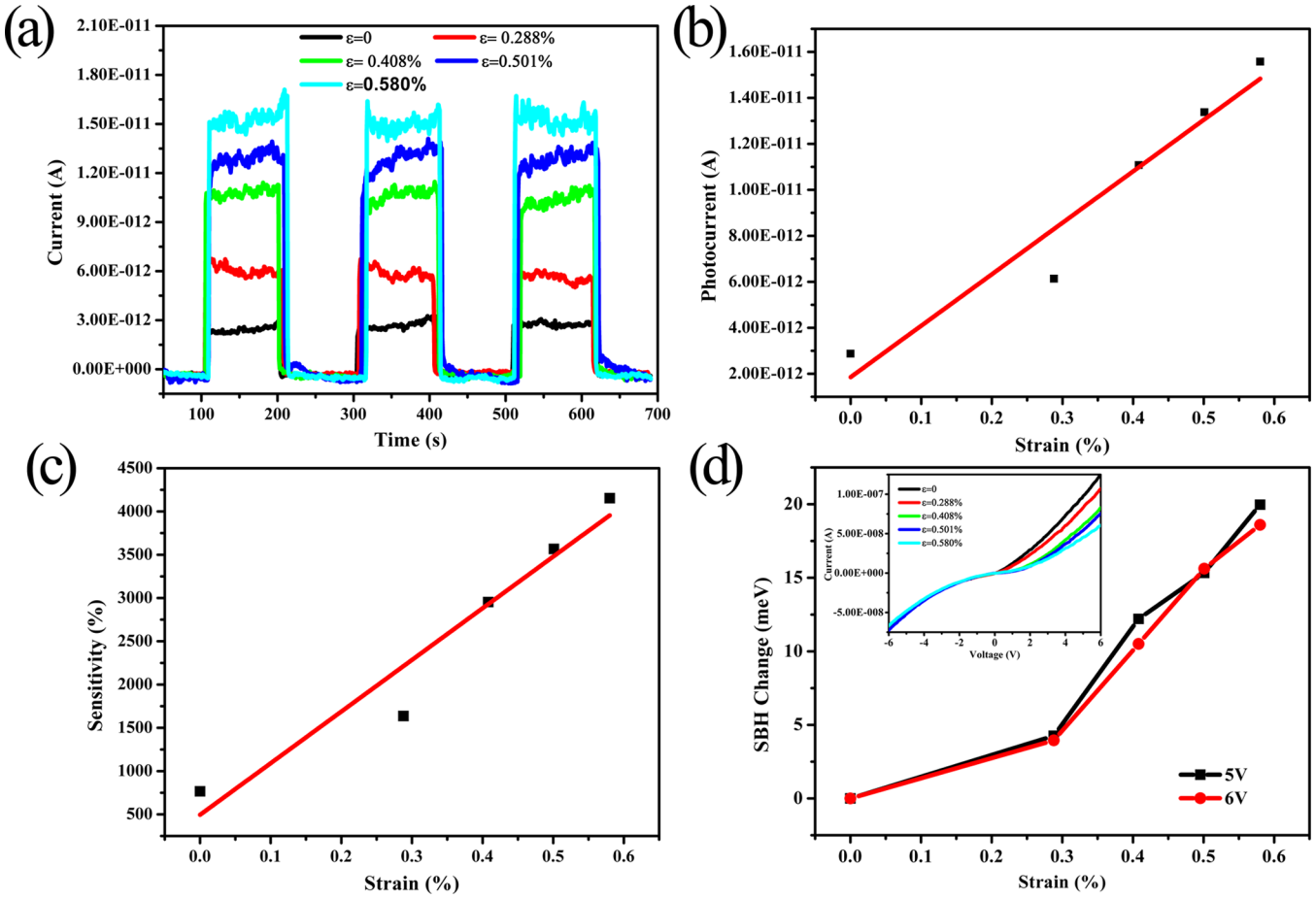

Figure 3. (a) Strain effect on the photoresponse characteristics. (b) Photocurrent and (c) sensitivity as a function of strain. (d) Derived SBH change with variable strains; (inset) *I*−*V* characteristics under different strains.

Figure 3a. These values are plotted in Figure 3, panels b and c, respectively, considering the minute variable of dark current. Both the photocurrent and the sensitivity increase linearly with increased tensile strain, and a 440% increase of photocurrent, together with a more than 5× enhancement of sensitivity, was obtained when applying a 0.580% tensile strain. It is worth noting that the enhanced photoresponse under strain does not influence the response time, stability, or repeatability of the device. To reveal the reason for the strain-enhanced performance of the device, we show the *I*−*V* curves with application of varying tensile strain to deduce the change of Schottky barrier height (SBH) under different tensile strains with different bias according to the classic thermionic emission−diffusion theory, as presented in Figure 3d. As expected, the change of Schottky barrier increases monotonically with the increased tensile strain, which is insensitive to external bias. It could be fairly verified that the optimized SBH could prompt the separation and extraction of the photogenerated electron−hole pairs and thus enhance the characteristic of the device due to the consistency of the variation trend between the change of SBH and photocurrent under strains.

The underlying mechanisms of the enhanced photoresonse of the device under strain could be clarified in the light of the realignment of their energy band diagram under strain. It is widely accepted that once the ZnO wire is strained, charge would redistribute to screen the piezoelectric charges partially as a result of the piezoelectric polarization charges arisen from its noncentral symmetric crystal structure, and the remnant piezopotential would modify the interface characteristics.[42] By utilizing the remnant piezopotential, the charge transport behavior at the interface is effectively modulated .[12−16] In our scenario, a negative piezopotential was produced at the MS interface, repelling electrons away from the interface and consequently further depleting the interface and raising the barrier height. The corresponding band diagram is plotted in Figure 4a. Undoubtedly, the stronger and expanding built-in field is favorable for the photoexcites separation and extraction. Though the piezoresistance effect would certainly take place and contribute to the charge transport behavior, it is a symmetrical effect that changes the conductance of the semiconductor instead of the interface characteristic. Therefore, the piezoelectric effect dominates the overall charge transport behavior in this work for the asymmetrical variation of current under positive and negative bias, which is shown in the inset of Figure 3d.

In addition, because the polarity of the piezopotential depends on the relationship between the direction of the *c*-axis of the ZnO wire and that of the applied strain, when the *c*-axis of ZnO points toward the epoxy, a positive piezopotential appears at the interface under tensile strain (Figure 4b), which causes electrons to accumulate at the interface, resulting in a narrower depletion layer and a lower barrier height. The shrunken and blunter built-in potential renders the reduction of the driven force of the photoexcites, suppressing the separation and extraction of the photoexcites, and inferior photoresponse properties are thus forecasted. The corresponding results are

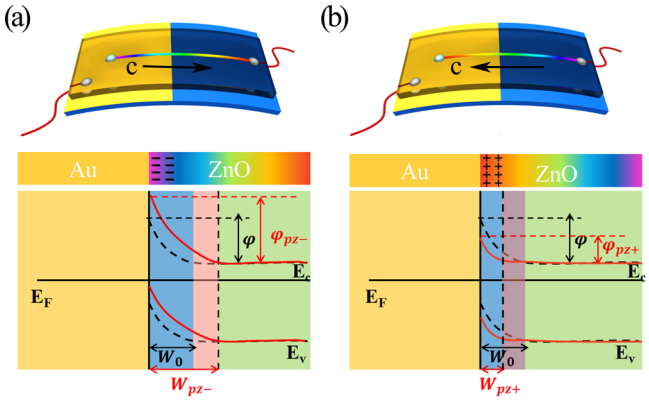

Figure 4. (Top) *c*-Axis of ZnO wire pointing (a) from epoxy to Ag electrode and (b) from Ag electrode to epoxy. (Bottom, a and b) Band diagram of ZnO/Au interface with and without strain, as shown in solid red and dotted black curves, respectively. W is the depletion width of the built-in field, and φ is the SBH.

exhibited in Figure 5. Expectedly, the photocurrent decreases with the increasing tensile strain, and the response time remains similarly invariable. Furthermore, a similar linear relationship between the photocurrent/sensitivity and tensile strain is also observed. The corresponding $I-V$ characteristics and calculated change of SBH under strains are presented in Figure 5d. The change of SBH decreases with increased tensile strains, which accounts for the weakened photoresponse.

CONCLUSION

In summary, with the interfacial piezopotential engineering induced stronger and expanding built-in field, the separation and extraction of the photoexcites at ZnO/Au interface was largely promoted, resulting in an enhanced photoresponse of the Schottky junction. The photocurrent increases linearly with applied tensile strain. A 440% enhancement of photocurrent and a 5× increase of sensitivity were achieved under a 0.580% tensile strain. The results provide guidance for designing and optimizing the performance of optoelectronics, which is applicable to self-powered systems involving piezoelectric semiconductor materials.

AUTHOR INFORMATION

Corresponding Author

*E-mail: yuezhang@ustb.edu.cn.

Notes

The authors declare no competing financial interest.

ACKNOWLEDGMENTS

This work was supported by the National Major Research Program of China (2013CB932602), the Program of International S&T Cooperation (2012DFA50990), NSFC (51232001,

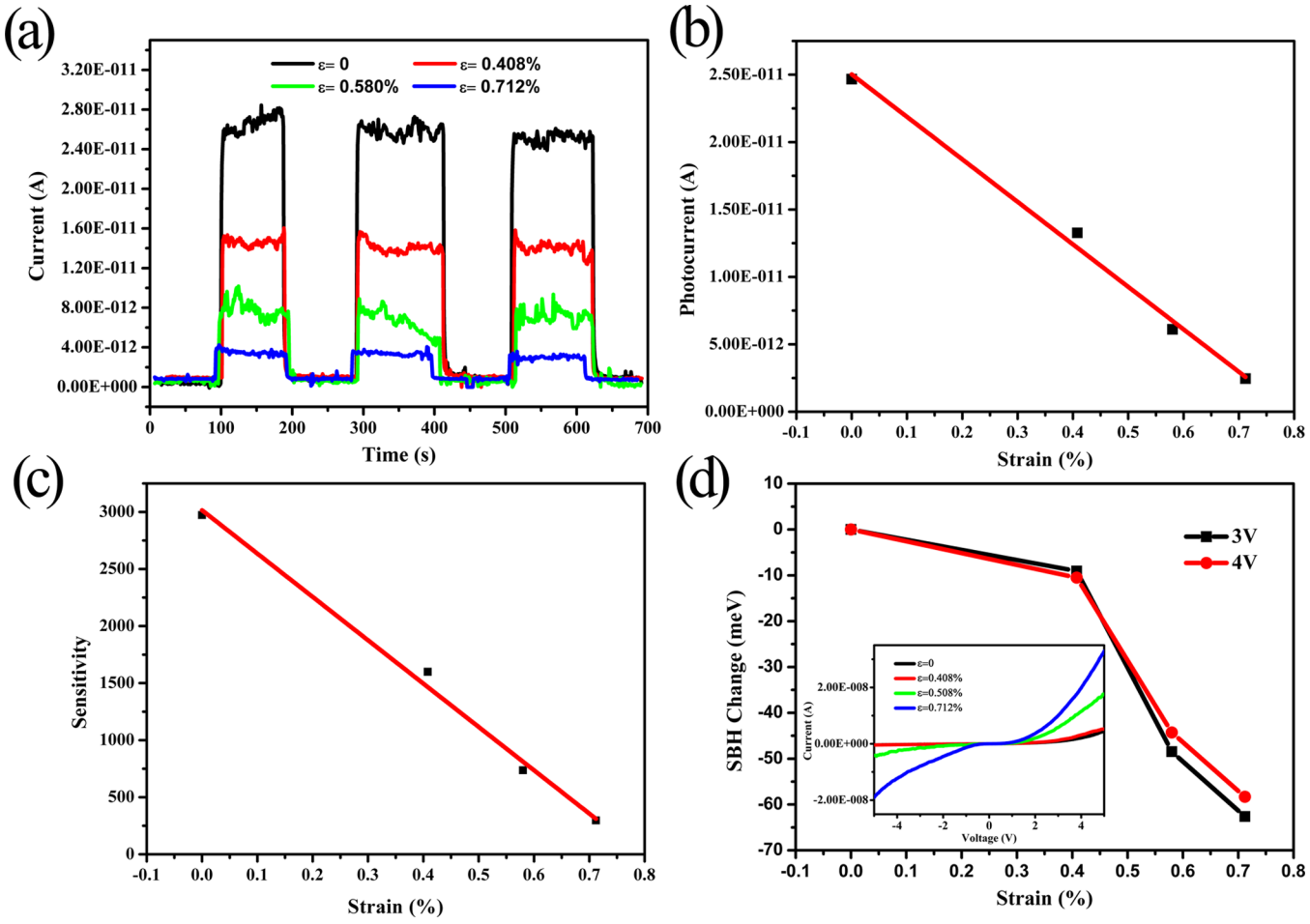

Figure 5. (a) Strain effect on the photoresponse characteristics. (b) Photocurrent and (c) sensitivity as a function of strain. (d) Derived SBH change with variable strains; (inset) $I-V$ characteristics under different strains.

51172022, and 51372020), the Research Fund of Co-Construction Program from the Beijing Municipal Commission of Education, the Fundamental Research Funds for the Central Universities, and the Program for Changjiang Scholars and Innovative Research Team in University.

REFERENCES

(1) Hammerl, G.; Spaldin, N. Shedding Light on Oxide Interfaces. *Science* **2011**, *332*, 922−923.
(2) Zubko, P.; Gariglio, S.; Gabay, M.; Ghosez, P.; Triscone, J.-M. Interface Physics in Complex Oxide Heterostructures. *Annu. Rev. Condens. Matter Phys.* **2011**, *2*, 141−165.
(3) Nakagawa, N.; Hwang, H. Y.; Muller, D. A. Why Some Interfaces Cannot be Sharp. *Nat. Mater.* **2006**, *5*, 204−209.
(4) Xiao, D.; Zhu, W.; Ran, Y.; Nagaosa, N.; Okamoto, S. Interface Engineering of Quantum Hall Effects in Digital Transition Metal Oxide Heterostructures. *Nat. Commun.* **2011**, *2*, 596.
(5) Xu, Y.; Shi, J.; Lv, S.; Zhu, L.; Dong, J.; Wu, H.; Xiao, Y.; Luo, Y.; Wang, S.; Li, D.; Li, X.; Meng, Q. Simple Way to Engineer Metal−Semiconductor Interface for Enhanced Performance of Perovskite Organic Lead Iodide Solar Cells. *ACS Appl. Mater. Interfaces* **2014**, *6*, 5651−5656.
(6) Wang, R.; Wang, S.; Zhang, D.; Li, Z.; Fang, Y.; Qiu, X. Control of Carrier Type and Density in Exfoliated Graphene by Interface Engineering. *ACS Nano* **2011**, *5*, 408−412.
(7) Liao, Q.; Zhang, Z.; Zhang, X.; Mohr, M.; Zhang, Y.; Fecht, H.-J. Flexible Piezoelectric Nanogenerators based on Fiber/ZnO Nanowires/Paper Hybrid Structure for Energy Harvesting. *Nano Res.* **2014**, *7*, 917−928.
(8) Yuan, Y.; Reece, T. J.; Sharma, P.; Poddar, S.; Ducharme, S.; Gruverman, A.; Yang, Y.; Huang, J. Efficiency Enhancement in Organic Solar Cells with Ferroelectric Polymers. *Nat. Mater.* **2011**, *10*, 296−302.
(9) Yang, B.; Yuan, Y.; Sharma, P.; Poddar, S.; Korlacki, R.; Ducharme, S.; Gruverman, A.; Saraf, R.; Huang, J. Tuning the Energy Level Offset between Donor and Acceptor with Ferroelectric Dipole Layers for Increased Efficiency in Bilayer Organic Photovoltaic Cells. *Adv. Mater.* **2012**, *24*, 1455−1460.
(10) Yu, R.; Pan, C.; Hu, Y.; Li, L.; Liu, H.; Liu, W.; Chua, S.; Chi, D.; Wang, Z. L. Enhanced Performance of GaN Nanobelt-Based Photodetectors by Means of Piezotronic Effects. *Nano Res.* **2013**, *6*, 758−766.
(11) Guo, W.; Yang, Y.; Qi, J.; Zhao, J.; Zhang, Y. Localized Ultraviolet Photoresponse in Single Bent ZnO Micro/Nanowires. *Appl. Phys. Lett.* **2010**, *97*, 133112.
(12) Wang, R.-C.; Lin, H.-Y.; Wang, C.-H.; Liu, C.-P. Fabrication of a Large-Area Al-Doped ZnO Nanowire Array Photosensor with Enhanced Photoresponse by Straining. *Adv. Funct. Mater.* **2012**, *22*, 3875−3881.
(13) Shi, J.; Zhao, P.; Wang, X. Piezoelectric-Polarization-Enhanced Photovoltaic Performance in Depleted-Heterojunction Quantum-Dot Solar Cells. *Adv. Mater.* **2013**, *25* (6), 916−921.
(14) Lin, P.; Yan, X.; Zhang, Z.; Shen, Y.; Zhao, Y.; Bai, Z.; Zhang, Y. Self-Powered UV Photosensor based on PEDOT:PSS/ZnO Micro/Nanowire with Strain-Modulated Photoresponse. *ACS Appl. Mater. Interfaces* **2013**, *5*, 3671−3676.
(15) Shoaee, S.; Briscoe, J.; Durrant, J. R.; Dunn, S. Acoustic Enhancement of Polymer/ZnO Nanorod Photovoltaic Device Performance. *Adv. Mater.* **2014**, *26*, 263−268.
(16) Pan, C.; Dong, L.; Zhu, G.; Niu, S.; Yu, R.; Yang, Q.; Liu, Y.; Wang, Z. L. High-Resolution Electroluminescent Imaging of Pressure Distribution Using a Piezoelectric Nanowire LED Array. *Nat. Photonics* **2013**, *7*, 752−758.
(17) Zhang, Y.; Yan, X.; Yang, Y.; Huang, Y.; Liao, Q.; Qi, J. Scanning Probe Study on the Piezotronic Effect in ZnO Nanomaterials and Nanodevices. *Adv. Mater.* **2012**, *24*, 4647−4655.
(18) Wang, Z. L.; Wu, W. Piezotronics and Piezo-Phototronics: Fundamentals and Applications. *Natl. Sci. Rev.* **2013**, *1*, 62−90.
(19) Yang, Y.; Qi, J.; Guo, W.; Gu, Y.; Huang, Y.; Zhang, Y. Transverse Piezoelectric Field-Effect Transistor based on Single ZnO Nanobelts. *Phys. Chem. Chem. Phys.* **2010**, *12*, 12415−12419.
(20) Yang, Q.; Guo, X.; Wang, W.; Zhang, Y.; Xu, S.; Lien, D. H.; Wang, Z. L. Enhancing Sensitivity of a Single ZnO Micro-/Nanowire Photodetector by Piezo-Phototronic Effect. *ACS Nano* **2010**, *4*, 6285−6291.
(21) Tsukazaki, A.; Ohtomo, A.; Onuma, T.; Ohtani, M.; Makino, T.; Sumiya, M.; Ohtani, K.; Chichibu, S. F.; Fuke, S.; Segawa, Y.; Ohno, H.; Koinuma, H.; Kawasaki, M. Repeated Temperature Modulation Epitaxy for P-type Doping and Light-Emitting Diode based on ZnO. *Nat. Mater.* **2004**, *4*, 42−46.
(22) Lévy-Clément, C.; Tena-Zaera, R.; Ryan, M. A.; Katty, A.; Hodes, G. CdSe-Sensitized p-CuSCN/Nanowire n-ZnO Heterojunctions. *Adv. Mater.* **2005**, *17*, 1512−1515.
(23) Johnson, J. C.; Yan, H.; Yang, P.; Saykally, R. J. Optical Cavity Effects in ZnO Nanowire Lasers and Waveguides. *J. Phys. Chem. B* **2003**, *107*, 8816−8828.
(24) Wang, W.; Qi, J.; Wang, Q.; Huang, Y.; Liao, Q.; Zhang, Y. Single ZnO Nanotetrapod-Based Sensors for Monitoring Localized UV Irradiation. *Nanoscale* **2013**, *5*, 5981−5985.
(25) Patra, D.; Sengupta, S.; Duan, W.; Zhang, H.; Pavlick, R.; Sen, A. Intelligent, Self-Powered, Drug Delivery Systems. *Nanoscale* **2013**, *5*, 1273−1283.
(26) Meng, B.; Tang, W.; Too, Z.-H.; Zhang, X.; Han, M.; Liu, W.; Zhang, H. A Transparent Single-Friction-Surface Triboelectric Generator and Self-Powered Touch Sensor. *Energy Environ. Sci.* **2013**, *6*, 3235−3240.
(27) Bie, Y. Q.; Liao, Z. M.; Zhang, H. Z.; Li, G. R.; Ye, Y.; Zhou, Y. B.; Xu, J.; Qin, Z. X.; Dai, L.; Yu, D. P. Self-Powered, Ultrafast, Visible-Blind UV Detection and Optical Logical Operation Based on ZnO/GaN Nanoscale P-N Junctions. *Adv. Mater.* **2011**, *23*, 649−653.
(28) Bai, S.; Xu, Q.; Gu, L.; Ma, F.; Qin, Y.; Wang, Z. L. Single Crystalline Lead Zirconate Titanate (PZT) Nano/Micro-Wire based Self-Powered UV Sensor. *Nano Energy* **2012**, *1*, 789−795.
(29) Gao, Z.; Jin, W.; Zhou, Y.; Dai, Y.; Yu, B.; Liu, C.; Xu, W.; Li, Y.; Peng, H.; Liu, Z.; Dai, L. Self-Powered Flexible and Transparent Photovoltaic Detectors based on CdSe Nanobelt/Graphene Schottky Junctions. *Nanoscale* **2013**, *5*, 5576−5581.
(30) Wu, D.; Jiang, Y.; Zhang, Y.; Yu, Y.; Zhu, Z.; Lan, X.; Li, F.; Wu, C.; Wang, L.; Luo, L. Self-Powered and Fast-Speed Photodetectors based on CdS:Ga Nanoribbon/Au Schottky Diodes. *J. Mater. Chem.* **2012**, *22*, 23272−23276.
(31) Yang, Y.; Guo, W.; Qi, J.; Zhao, J.; Zhang, Y. Self-powered Ultraviolet Photodetector based on a Single Sb-Doped ZnO Nanobelt. *Appl. Phys. Lett.* **2010**, *97*, 223113.
(32) Hassan, J. J.; Mahdi, M. A.; Kasim, S. J.; Ahmed, N. M.; Abu Hassan, H.; Hassan, Z. High Sensitivity and Fast Response and Recovery Times in a ZnO Nanorod Array/p-Si Self-Powered Ultraviolet Detector. *Appl. Phys. Lett.* **2012**, *101*, 261108.
(33) Ni, P.-N.; Shan, C.-X.; Wang, S.-P.; Liu, X.-Y.; Shen, D.-Z. Self-Powered Spectrum-Selective Photodetectors Fabricated from n-ZnO/p-NiO Core−Shell Nanowire Arrays. *J. Mater. Chem. C* **2013**, *1*, 4445−4449.
(34) Hatch, S. M.; Briscoe, J.; Dunn, S. A Self-Powered ZnO-Nanorod/CuSCN UV Photodetector Exhibiting Rapid Response. *Adv. Mater.* **2013**, *25*, 867−871.
(35) Game, O.; Singh, U.; Kumari, T.; Banpurkar, A.; Ogale, S. ZnO(N)-Spiro-MeOTAD Hybrid Photodiode: An Efficient Self-Powered Fast-Response UV (Visible) Photosensor. *Nanoscale* **2014**, *6*, 503−513.
(36) Huang, Y. H.; Zhang, Y.; Liu, L.; Fan, S. S.; Wei, Y.; He, J. Controlled Synthesis and Field Emission Properties of ZnO Nanostructures with Different Morphologies. *J. Nanosci. Nanotechnol.* **2006**, *6*, 787−790.
(37) Willander, M.; Yang, L. L.; Wadeasa, A.; Ali, S. U.; Asif, M. H.; Zhao, Q. X.; Nur, O. Zinc Oxide Nanowires: Controlled Low Temperature Growth and Some Electrochemical and Optical Nano-devices. *J. Mater. Chem.* **2009**, *19*, 1006−1018.

(38) Djurisic, A. B.; Leung, Y. H. Optical Properties of ZnO Nanostructures. *Small* **2006**, *2*, 944−961.
(39) Brötzmann, M.; Vetter, U.; Hofsäss, H. BN/ZnO Heterojunction Diodes with Apparently Giant Ideality Factors. *J. Appl. Phys.* **2009**, *106*, 063704.
(40) Pal, B. N.; Robel, I.; Mohite, A.; Laocharoensuk, R.; Werder, D. J.; Klimov, V. I. High-Sensitivity P-N Junction Photodiodes Based on PbS Nanocrystal Quantum Dots. *Adv. Funct. Mater.* **2012**, *22*, 1741−1748.
(41) Hu, Y.; Klein, B. D.; Su, Y.; Niu, S.; Liu, Y.; Wang, Z. L. Temperature Dependence of the Piezotronic Effect in ZnO Nanowires. *Nano Lett.* **2013**, *13*, 5026−5032.
(42) Shi, J.; Starr, M. B.; Wang, X. Band Structure Engineering at Heterojunction Interfaces via the Piezotronic Effect. *Adv. Mater.* **2012**, *24*, 4683−4691.